resistant human immunodeficiency virus type 1 protease reveal an expanded active-site cavity. *J. Virol.* 78(6), 3123–3132.

Markowitz, M., Mo, H., Kempf, D. J., Norbeck, D. W., Bhat, T. N., Erickson, J. W., and Ho, D. D. (1995). Selection and analysis of human immunodeficiency virus type 1 variants with increased resistance to ABT-538, a novel protease inhibitor. *J. Virol.* 69, 701–706.

Mitsuya, H., and Broder, S. (1986). Inhibition of the *in vitro* infectivity and cytopathic effect of human T-lymphotropic virus type III/lymphadenopathy virus-associated virus (HTLV-III/LAV) by 2′,3′-dideoxynucleosides. *Proc. Natl. Acad. Sci. USA* 83, 1911–1915.

Mitsuya, H., and Broder, S. (1987). Strategies for antiviral therapy in AIDS. *Nature* 325, 773–778.

Mitsuya, H., and Erickson, J. (1999). Discovery and development of antiretroviral therapeutics for HIV infection. *In* "Textbook of AIDS Medicine" (T. C. Merigan, J. G. Bartlet, and D. Bolognesi, Eds.), pp. 751–780. Williams & Wilkins, Baltimore.

Mitsuya, H., Weinhold, K. J., Furman, P. A., St Clair, M. H., Nusinoff Lehrman, S., Gallo, R. C., Bolognesi, D., Barry, D. W., and Broder, S. (1985). 3′-Azido-3′-deoxythymidine (BW A509U): An antiviral agent that inhibits the infectivity and cytopathic effect of human T-lymphotropic virus type III/lymphadenopathy-associated virus *in vitro*. *Proc. Natl. Acad. Sci. USA* 82, 7096–7100.

Mitsuya, H., Yarchoan, R., and Broder, S. (1990). Molecular targets for AIDS therapy. *Science* 249, 1533–1544.

Molla, A., Korneyeva, M., Gao, Q., Vasavanonda, S., Schipper, P. J., Mo, H. M., Markowitz, M., Chernyavskiy, T., Niu, P., Lyons, N., Hsu, A., Granneman, G. R., *et al.* (1996). Ordered accumulation of mutations in HIV protease confers resistance to ritonavir. *Nat. Med.* 2(7), 760–766.

Muzammil, S., Kang, L. W., Armstrong, A. A., Jakalian, A., Bonneau, P. R., Schmelmer, V., Amzel, L. M., and Freire, E. (2005). Unique response of tipranavir to multi-drug resistant HIV-1 protease suggests new ways of combating drug resistance. *Antiviral Res.* 10(S70), Abstract 63.

Ohtaka, H., and Freire, E. (2005). Adaptive inhibitors of the HIV-1 protease. *Prog. Biophys. Mol. Biol.* 88(2), 193–208.

Otto, M. J., Garber, S., Winslow, D. L., Reid, C. D., Aldrich, P., Jadhav, P. K., Patterson, C. E., Hodge, C. N., and Cheng, Y. S. (1993). *In vitro* isolation and identification of human immunodeficiency virus (HIV) variants with reduced sensitivity to C-2 symmetrical inhibitors of HIV type 1 protease. *Proc. Natl. Acad. Sci. USA* 90(16), 7543–7547.

Overington, J. P., Al-Lazikani, B., and Hopkins, A. L. (2006). How many drug targets are there? *Nat. Rev. Drug Discov.* 5, 993–996.

Peters, S., Munoz, M., Yerly, S., Sanchez-Merino, V., Lopez-Galindez, C., Perrin, L., Larder, B., Cmarko, D., Fakan, S., Meylan, P., and Telenti, A. (2001). Resistance to nucleoside analog reverse transcriptase inhibitors mediated by human immunodeficiency virus type 1 p6 protein. *J. Virol.* 75(20), 9644–9653.

Poppe, S. M., Slade, D. E., Chong, K. T., Hinshaw, R. R., Pagano, P. J., Markowitz, M., Ho, D. D., Mo, H., Gorman, R. R., 3rd, Dueweke, T. J., Thaisrivongs, S., and Tarpley, W. G. (1997). Antiviral activity of the dihydropyrone PNU-140690, a new nonpeptidic human immunodeficiency virus protease inhibitor. *Antimicrob. Agents Chemother.* 41(5), 1058–1063.

Prabu-Jeyabalan, M., Nalivaika, E., and Schiffer, C. A. (2000). How does a symmetric dimer recognize an asymmetric substrate? A substrate complex of HIV-1 protease. *J. Mol. Biol.* 301(5), 1207–1220.

Prabu-Jeyabalan, M., Nalivaika, E., and Schiffer, C. A. (2002). Substrate shape determines specificity of recognition for HIV-1 protease: Analysis of crystal structures of six substrate complexes. *Structure* 10(3), 369–381.

Prabu-Jeyabalan, M., Nalivaika, E. A., King, N. M., and Schiffer, C. A. (2003). Viability of a drug-resistant human immunodeficiency virus type 1 protease variant: Structural insights for better antiviral therapy. *J. Virol.* 77(2), 1306–1315.

Randolph, J. T., and DeGoey, D. A. (2004). Peptidomimetic inhibitors of HIV protease. *Curr. Top. Med. Chem.* 4(10), 1079–1095.

Roberts, N. A., Martin, J. A., Kinchington, D., Broadhurst, A. V., Craig, J. C., Duncan, I. B., Galpin, S. A., Handa, B. K., Kay, J., and Krohn, A. (1990). Rational design of peptide-based HIV proteinase inhibitors. *Science* 248, 358–361.

Rusconi, S., La Seta Catamancio, S., Citterio, P., Kurtagic, S., Violin, M., Balotta, C., Moroni, M., Galli, M., and d'Arminio-Monforte, A. (2000). Susceptibility to PNU-140690 (Tipranavir) of human immunodeficiency virus type 1 isolates derived from patients with multidrug resistance to other protease inhibitors. *Antimicrob. Agents Chemother.* 44(5), 1328–1332.

Schake, D. (2004). How flexible is tipranavir in complex with the HIV-1 protease active site? *AIDS* 18(3), 579–580.

Schake, D. (2005). Molecular significance of tipranavir related codon 33 protease gene mutations. *AIDS* 19(2), 218–219.

Siliciano, J. D., Siliciano, R. F., Blankson, J. N., Persaud, D., Siliciano, R. F., Pierson, T., McArthur, J., Siliciano, R. F., and Siliciano, R. (2004). A long-term latent reservoir for HIV-1: Discovery and clinical implications. *J. Antimicrob. Chemother.* 54(1), 6–9.

Simon, V., and Ho, D. D. (2003). HIV-1 dynamics *in vivo*: Implications for therapy. *Nat. Rev. Microbiol.* 1(3), 181–190.

Sommadossi, J. P. (1999). HIV protease inhibitors: Pharmacologic and metabolic distinctions. *AIDS* 13(Suppl. 1), S29–S40.

Surleraux, D. L., de Kock, H. A., Verschueren, W. G., Pille, G. M., Maes, L. J., Peeters, A., Vendeville, S., De Meyer, S., Azijn, H., Pauwels, R., de Bethune, M. P., King, N. M., *et al.* (2005a). Design of HIV-1 protease inhibitors active on multidrug-resistant virus. *J. Med. Chem.* 48(6), 1965–1973.

Surleraux, D. L., Tahri, A., Verschueren, W. G., Pille, G. M., de Kock, H. A., Jonckers, T. H., Peeters, A., De Meyer, S., Azijn, H., Pauwels, R., de Bethune, M. P., King, N. M., *et al.* (2005b). Discovery and selection of TMC114, a next generation HIV-1 protease inhibitor. *J. Med. Chem.* 48(6), 1813–1822.

Tamiya, S., Mardy, S., Kavlick, M. F., Yoshimura, K., and Mitsuya, H. (2004). Amino acid insertions near Gag cleavage sites restore the otherwise compromised replication of human immunodeficiency virus type 1 variants resistant to protease inhibitors. *J. Virol.* 78(21), 12030–12040.

Tanaka, M., Srinivas, R. V., Ueno, T., Kavlick, M. F., Hui, F. K., Fridland, A., Driscoll, J. S., and Mitsuya, H. (1997). *In vitro* induction of human immunodeficiency virus type 1 variants resistant to 2′-beta-Fluoro-2′,3′-dideoxyadenosine. *Antimicrob. Agents Chemother.* 41(6), 1313–1318.

Tie, Y., Boross, P. I., Wang, Y. F., Gaddis, L., Hussain, A. K., Leshchenko, S., Ghosh, A. K., Louis, J. M., Harrison, R. W., and Weber, I. T. (2004). High resolution crystal structures of HIV-1 protease with a potent non-peptide inhibitor (UIC-94017) active against multi-drug-resistant clinical strains. *J. Mol. Biol.* 338(2), 341–352.

Tisdale, M., Myers, R. E., Maschera, B., Parry, N. R., Oliver, N. M., and Blair, E. D. (1995). Cross-resistance analysis of human immunodeficiency virus type 1 variants individually selected for resistance to five different protease inhibitors. *Antimicrob. Agents Chemother.* 39(8), 1704–1710.

Turk, B. (2006). Targeting proteases: Successes, failures and future prospects. *Nat. Rev. Drug Discov.* 5, 785–799.

Turner, S. R., Strohbach, J. W., Tommasi, R. A., Aristoff, P. A., Johnson, P. D., Skulnick, H. I., Dolak, L. A., Seest, E. P., Tomich, P. K., Bohanon, M. J., Horng, M. M., Lynn, J. C., *et al.* (1998). Tipranavir (PNU-140690): A potent, orally bioavailable nonpeptidic HIV

protease inhibitor of the 5,6-dihydro-4-hydroxy-2-pyrone sulfonamide class. *J. Med. Chem.* 41(18), 3467–3476.

Ward, D., Lalezari, J., Thompson, M., Dejesus, E., Lamarca, A., Hawkins, T., Green, S., Myers, R., Ford, S., Ng-Cashin, J., Stclair, M., Reddy, S., *et al.* (2005). Preliminary Antiviral Activity and Safety of 640385/Ritonavir in HIV-infected Patients (Study HPR10006); an 8-Week Interim Analysis. *In* "45th Interscience Conference on Antimicrobial Agents and Chemotherapy, Washington DC.", Abstract H-412.

Watkins, T., Resch, W., Irlbeck, D., and Swanstrom, R. (2003). Selection of high-level resistance to human immunodeficiency virus type 1 protease inhibitors. *Antimicrob. Agents Chemother.* 47(2), 759–769.

Winters, M. A., Coolley, K. L., Girard, Y. A., Levee, D. J., Hamdan, H., Shafer, R. W., Katzenstein, D. A., and Merigan, T. C. (1998). A 6-basepair insert in the reverse transcriptase gene of human immunodeficiency virus type 1 confers resistance to multiple nucleoside inhibitors. *J. Clin. Invest.* 102(10), 1769–1775.

Yarchoan, R., Mitsuya, H., Thomas, R. V., Pluda, J. M., Hartman, N. R., Perno, C. F., Marczyk, K. S., Allain, J. P., Johns, D. G., and Broder, S. (1989a). *In vivo* activity against HIV and favorable toxicity profile of 2′,3′-dideoxyinosine. *Science* 245, 412–415.

Yarchoan, R., Mitsuya, H., Myers, C. E., and Broder, S. (1989b). Clinical pharmacology of 3′-azido-2′,3′-dideoxythymidine (zidovudine) and related dideoxynucleosides. *N. Engl. J. Med.* 321, 726–738.

Yarchoan, R., Lietzau, J. A., Nguyen, B. Y., Brawley, O. W., Pluda, J. M., Saville, M. W., Wyvill, K. M., Steinberg, S. M., Agbaria, R., Mitsuya, H., and Broder, S. (1994). A randomized pilot study of alternating or simultaneous zidovudine and didanosine therapy in patients with symptomatic human immunodeficiency virus infection. *J. Infect. Dis.* 169 (1), 9–17.

Yates, P., Hazen, R., St Clair, M., Boone, L., and Elston, R. (2004). *In vitro* selection and characterisation of resistance to the new HIV protease inhibitor GW640385. *Antivir. Ther.* 9(S16), 12.

Yin, P. D., Das, D., and Mitsuya, H. (2006). Overcoming HIV drug resistance through rational drug design based on molecular, biochemical, and structural profiles of HIV resistance. *Cell. Mol. Life Sci.* 63, 1706–1724.

Yoshimura, K., Kato, R., Kavlick, M. F., Nguyen, A., Maroun, V., Maeda, K., Hussain, K. A., Ghosh, A. K., Gulnik, S. V., Erickson, J. W., and Mitsuya, H. (2002). A potent human immunodeficiency virus type 1 protease inhibitor, UIC-94003 (TMC-126), and selection of a novel (A28S) mutation in the protease active site. *J. Virol.* 76(3), 1349–1358.

Yusa, K., and Harada, S. (2004). Acquisition of multi-PI (protease inhibitor) resistance in HIV-1 *in vivo* and *in vitro*. *Curr. Pharm. Des.* 10(32), 4055–4064.

Zhang, Y. M., Imamichi, H., Imamichi, T., Lane, H. C., Falloon, J., Vasudevachari, M. B., and Salzman, N. P. (1997). Drug resistance during indinavir therapy is caused by mutations in the protease gene and in its Gag substrate cleavage sites. *J. Virol.* 71(9), 6662–6670.

Parasite Immunology, 2008, **30**, 13–21 DOI: 10.1111/j.1365-3024.2007.00988.x

Recognition profiles of microsporidian *Encephalitozoon cuniculi* polar tube protein 1 with human immunoglobulin M antibodies

K. FURUYA,[1] M. OMURA,[1] S. KUDO,[2] W. SUGIURA[3] & H. AZUMA[4]

[1]Department of Parasitology, National Institute of Infectious Diseases, Tokyo, Japan, [2]Hokkaido Institute of Public Health, Sapporo, Japan, [3]AIDS Research Center, National Institute of Infectious Diseases, Tokyo, Japan, [4]Hokkaido Red Cross Blood Center, Sapporo, Japan

SUMMARY

Microsporidian Encephalitozoon cuniculi *has a unique organelle called a polar tube (PT), the extrusion of which is absolutely required to invade a host cell. We recently detected anti-*E. cuniculi *PT immunoglobulin (Ig) M antibodies in sera from many healthy individuals. The present one-dimensional (1-D) immunoblot analysis predominantly detected a band at 52 kDa in all of the examined human sera with anti-PT IgM. The use of mouse monoclonal antibody confirmed that the 52-kDa band detected in 1-D immunoblots was an antigen derived from the PT, which represents a glycoprotein nature. In addition, from changes in the immunoreactivity of the 52-kDa band before and after treatment with NaOH, we determined that the 24 human serum samples with anti-PT IgM activities could be roughly grouped into three types: (i) sera containing antibodies against only a saccharic determinant (n = 3); (ii) sera containing antibodies against only a proteinic determinant (n = 11); and (iii) sera showing dual recognition of saccharic and proteinic determinants (n = 10). Further two-dimensional (2-D) immunoblot analysis followed by proteomic analysis confirmed that human sera with anti-PT IgM reacted with* E. cuniculi *polar tube protein 1 (PTP1). Such circulating IgM antibodies may be important in the first line of defence against* E. cuniculi *infection.*

Keywords *antigenic determinant,* Encephalitozoon cuniculi, *human IgM antibody, Microsporidia, polar tube*

Correspondence: K. Furuya, Department of Parasitology, National Institute of Infectious Diseases, 1-23-1 Toyama, Shinjuku-ku, Tokyo 162-8640, Japan (e-mail: kfuruya@nih.go.jp).
Received: 17 July 2007
Accepted for publication: 14 September 2007

INTRODUCTION

Encephalitozoon cuniculi is a spore-forming obligate intracellular parasitic pathogen belonging to the phylum Microsporidia (1); it can also be a zoonotic parasite (2). Various animals can be naturally infected by *E. cuniculi* and humans can also be affected by this pathogen (3). However, most *E. cuniculi* infections occur in human immunodeficiency virus (HIV)-infected immunocompromised patients (2,4). A few cases of *E. cuniculi* infection have also been reported in transplant patients (2,5,6). Apart from an accidentally infected French individual who had severe keratoconjunctivitis (7), no symptomatic cases of infection with *E. cuniculi* among immunocompetent persons have been described (2,4). Thus, it is most unlikely that *E. cuniculi* causes microsporidiosis in immunocompetent persons (2,4). In humans, it can be regarded as an opportunistic pathogen (8,9).

We recently demonstrated immunoglobulin (Ig) M antibodies against the polar tubes (PTs) of *E. cuniculi* in about 36% of healthy people in Japan (10); by contrast, such IgM antibodies were poorly detected among HIV-positive persons. The rate of positivity for anti-PT IgM was significantly reduced with increasing age and decreasing CD4 cell count. These seroepidemiological results clearly indicate that circulating anti-PT IgM antibodies that are capable of strongly reacting with filaments extruded from germinated spores exist, thus suggesting that such antibodies may play a part in protective immunity.

The main objectives of this study were to provide further information about the immunoreactivity of human anti-PT IgM and to identify the corresponding determinants using one-dimensional (1-D) and two-dimensional (2-D) immunoblot analyses, and other biochemical and proteomic means.

MATERIALS AND METHODS

Serum samples

Twenty-four human serum samples were used for this study. These samples were collected from healthy individuals

under the ethical considerations described in a previous study (10).

As the positive control, serum samples from 11 infected rabbits were also used for this study. All the rabbits were sacrificed after approval from the breeding owners and were microbiologically confirmed to carry the pathogen in organs such as the brain and kidney. Isolated *E. cuniculi* spores from the organs were identified by polymerase chain reaction, as described before (11). The internal transcribed spacer gene sequence revealed that the *E. cuniculi* isolates were all classified into genotype 1.

In addition, 11 normal rabbit serum samples, which were serologically negative, were used as the negative control.

Mouse monoclonal antibody

A mouse monoclonal antibody against the soluble antigen of *E. cuniculi* PTs was generated using a hybridoma technique (12), which was tentatively named MAb2 for this study. After the second cloning, culture supernatants containing MAb2 were employed in the present study. In a later study, monoclonal antibodies from mouse ascitic fluids were available and were classified as IgE (manuscript in preparation). To detect IgE in this study, we used goat anti-mouse IgG + M + A (H + L) and rabbit anti-mouse IgG (H + L), which were labelled with enzyme, as documented below. All the reagents used could detect IgE, since they are also specific for light chains.

Preparation of purified spores of *Encephalitozoon cuniculi*

Encephalitozoon cuniculi spores of strain HF (genotype 1) were collected from the culture supernatants of infected RK 13 cells and purified using Percoll gradient centrifugation, as described previously (10). Finally, separated spores were filtered through Ultrafree-MC membranes (5·0 μm; Millipore Corporation, Bedford, MA).

Enzyme-linked immunosorbent assay (ELISA)

As described in a previous paper (10), anti-*E. cuniculi* PT antibodies were measured using a 96-well flat-bottom microplate coated with germinated spores. Twofold dilutions of each serum sample, starting a 1 : 50 dilution, were tested; bound antibodies were detected by the secondary antibody labelled with peroxidase (PO). Signals of PO bound to human or animal antibodies were visualized using an aminoethyl carbazole substrate kit (Zymed Laboratories Inc., San Diego, CA). The following PO conjugates were used as the secondary antibodies: rabbit anti-human IgM (μ-chain specific; QED Bioscience, San Diego, CA) for human IgM; goat anti-mouse IgG + M + A (H + L; Zymed Laboratories) for mouse monoclonal antibody. Also, protein A/G–PO conjugate (Prozyme Inc., San Leandro, CA) and protein A–PO conjugate (Kirkegaard & Perry Laboratories, Gaithersburg, MD) were used for detecting human IgG and rabbit IgG, respectively. Dilutions of the second reagents were adjusted between 1 : 3000 and 1 : 5000.

1-D polyacrylamide gel electrophoresis (1-D PAGE)

Purified *E. cuniculi* spores were suspended in an appropriate volume of Laemmli sample buffer (Bio-Rad Laboratories, Hercules, CA) containing 5% 2-mercaptoethanol (Bio-Rad) and heated at 95°C for 5 min. After centrifugation at about 7800 *g* for 5 min, pellets were treated twice more with the same buffer and the three supernatants were pooled. The protein fraction of these pooled supernatants was desalted using a NAP-5 column (GE Healthcare Bio-Sciences AB, Uppsala, Sweden). This soluble protein fraction was used as an antigen for 1-D immunoblot analysis.

Approximately 60 μg of the microsporidial soluble fraction was electrophoresed vertically using 15% polyacrylamide Ready mini-gels (Bio-Rad) under reducing conditions.

1-D immunoblot analysis

Electrophoresed spore proteins separated by 1-D PAGE were transferred electrically onto polyvinylidene fluoride (PVDF) membranes (immobilon transfer membranes; Millipore Corporation). Blotted membranes were cut into strips of about 4-mm width. Half of the strips were treated with a 0·055 M NaOH solution for 16 h at 40°C to remove carbohydrate chains from glycoproteins, according to the method described by Duk *et al.* (13). NaOH-treated strips were washed extensively with pure water.

All of the strips to be tested were treated with blocking buffer (SuperBlock; Pierce Chemical Company, Rockford, IL) and subsequently incubated with human sera, rabbit sera or a culture supernatant containing MAb2. Dilutions of human sera, rabbit sera and the supernatant to be tested were 1 : 100. Secondary antibodies labelled with alkaline phosphatase (ALP) were used to detect primary antibodies: goat anti-human IgM (μ-chain specific; Kirkegaard & Perry Laboratories) for human IgM; goat anti-rabbit IgM (μ-chain specific; Southern Biotechnology Associates, Birmingham, AL) for rabbit IgM; rabbit anti-mouse IgG (H + L; Zymed Laboratories) for mouse monoclonal antibody. The secondary antibodies were used at dilutions of 1 : 1000–1 : 3000. Reactions with the primary antibodies and the secondary antibodies were performed for 90 min at room temperature with shaking. After extensive washing with phosphate-buffered saline containing 0·05% Tween 20 (PBS-T), antibody binding was detected using a BCIP/

NBT phosphatase substrate kit (Kirkegaard & Perry Laboratories).

For each human serum, mouse monoclonal antibody and rabbit serum, the change in immunoreactivity between a NaOH-treated strip and an untreated strip was observed. In addition, the participation of a saccharic determinant in an immunological reaction was determined.

Analysis of lectin–carbohydrate interactions

Using some of the NaOH-treated or NaOH-untreated strips described above, the reactivities of various biotinylated lectins were tested. For this test, a biotinylated lectin kit I (BK-1000; Vector Laboratories, Buringame, CA), containing concanavalin A (ConA), *Dolichos biflorus* agglutinin, peanut agglutinin, *Ricinus communis* agglutinin I, soybean agglutinin, *Ulex europaeus* agglutinin I and wheat germ agglutinin, was used. Blots were incubated in a 20 μg/mL solution of each biotinylated lectin, in accordance with the manufacturer's instructions, followed by a 1 : 5000 dilution of streptavidin–ALP conjugate (Molecular Probes Inc., Eugene, OR). A BCIP/NBT phosphatase substrate kit (Kirkegaard & Perry Laboratories) was employed for colour development.

2-D polyacrylamide gel electrophoresis (2-D PAGE)

To an approximately 5×10^8 spore pellet, a 5% sodium dodecyl sulphate (SDS) solution was added, and the suspension was boiled for 5 min. Proteins were precipitated by the addition of trichloroacetic acid at a final concentration of 10%, washed once with cold 90% acetone, and dissolved in sample buffer containing 8 M urea, 2% CHAPS, 1% 1,4-dithiothreitol (DTT; Wako Pure Chemical Industries, Osaka, Japan), and 0·5% Pharmalyte (pH 3–10; Amersham Biosciences AB, Uppsala, Sweden). To remove protein aggregates, the protein solution was centrifuged and the supernatants were used as samples for 2-D PAGE. Protein concentrations were measured using a 2D-Quant kit (Amersham).

Isoelectric focusing was performed using commercially available Immobiline DryStrip gels (7 cm, pH 3–10; Amersham). Samples (about 50 μg of spore protein) were loaded by rehydration for 15 h in a solution containing 8 M urea, 2% CHAPS, 1% DTT and 0·5% Pharmalyte (pH 3–10). Isoelectric focusing was performed using an Ettan IPGphor II IEF system (Amersham) for 11 519 Vh. Voltage profiles were chosen according to the manual provided with the system. After consecutive equilibration of gels in a 50 mM Tris–HCl (pH 8·8) solution containing 6 M urea, 30% glycerol, 2% SDS and 1% DTT for 15 min, separation in the second dimension was performed using a mini-gel (10 × 10 cm) electrophoresis system with 12·5% Ready gels (Biocraft Inc., Tokyo, Japan), at 20 mA/gel.

N-terminal peptide sequencing

After 2-D PAGE, blotted proteins were stained with BODIPY FL-X, SE (Molecular Probes). Protein spots corresponding to those recognized by serum samples were excised and subjected to N-terminal sequence analysis in a Procise 494 protein sequencer (Applied Biosystems, Foster City, CA). Edman degradation was performed according to a standard program supplied by Applied Biosystems. The amino acid sequences obtained were compared to those of known proteins in the GenomeNet BLAST2 NR-AA database using the Web-accessible FASTA search program.

LC-MS/MS analysis

Spots assigned to immunogenic proteins were also excised from 2-D gels as described above. Gel pieces were subjected to in-gel digestion using the procedure published by Hellman *et al.* (14). Briefly, the protein in each gel plug was reduced with 100 mM DTT for 30 min at 50°C, alkylated with 100 mM iodoacetamide (Wako Pure Chemical) for 30 min at 37°C, and digested with 25 ng/μL trypsin (Wako Pure Chemical) overnight at 37°C. Peptides were extracted from the gel by diffusion in a 50% acetonitrile solution containing 5% formic acid, vacuum-dried, and then reconstituted in 20 μL of 0·1% trifluoroacetic acid. Extracted peptides were loaded on a high-performance liquid chromatography system (LC; MAGIC2002, Michrom BioResources Co. Ltd, Auburn, CA), eluted using an acetic acid–acetonitrile gradient, and directly injected into an LCQ ion trap mass spectrometer (MS; LCQ-Deca XP, Thermo Electron Co. Ltd, San Jose, CA) fitted with a nanoelectrospray ionization source, and operated in the positive ion mode. MS/MS spectra were acquired using data-dependent scanning, processed using the SEQUEST software program, and then searched against the NCBI NR database.

2-D immunoblot analysis

Spore proteins separated by 2-D PAGE were transferred onto PVDF membranes (ProBlot membranes, Applied Biosystems). Blotted membranes were treated with blocking buffer (SuperBlock) overnight at 4°C. Representative human sera were used as primary antibodies at a dilution of 1 : 100. ALP-labelled anti-human IgM (μ-chain specific; Kirkegaard & Perry Laboratories) was used as a secondary antibody at a dilution of 1 : 1000. Reactions with the primary and secondary antibodies were performed for 2 and 1 h, respectively, at room temperature with shaking. After extensive washing with

PBS-T, antibody binding was detected using a BCIP/NBT phosphatase substrate kit (Kirkegaard & Perry Laboratories).

As a positive control, we used a pool of 11 sera from infected rabbits at a dilution of 1 : 400. In addition, a pool of 11 sera from normal rabbits was used as a negative control at the same dilution. A culture supernatant containing MAb2 monoclonal antibody was also used at a dilution of 1 : 100 for epitope analysis. To detect these primary antibodies, ALP-labelled protein A (Zymed Laboratories) and ALP-labelled rabbit anti-mouse IgG (H + L; Zymed Laboratories) were used for rabbit IgG and the monoclonal antibody, respectively, at a dilution of 1 : 1000.

RESULTS

Measurements of anti-PT antibodies in the ELISA test

Twenty-four human serum samples used for this study revealed anti-PT IgM activities at titres between 1 : 200 and 1 : 1600 in the ELISA test. Figure 1(a) shows filaments that are strongly immunostained with IgM antibodies in the serum H-168. All samples except for H-197 had IgG antibody activity for extruded filaments below 1 : 50. However, the positive signal of H-197 was very weak, even at lower dilutions, probably because of the use of protein A/G conjugate as a secondary antibody.

Figure 1(b) shows filaments immunostained with IgG antibodies in a rabbit serum, which was used as a positive control for ELISA testing. The culture supernatant showed monoclonal antibody (MAb2) weakly immunostained filaments when it was tested by ELISA (data not shown).

Immunoreactivity of human sera on 1-D blots before and after treatment with NaOH

All 24 human serum samples generated clearly positive signals of an IgM antibody on a band migrating at 52 kDa in the 1-D immunoblot analysis without NaOH treatment (Figure 2; odd-numbered strips). Besides the positive signals for this 52-kDa band, which was MAb2-positive (strip P1), most sera also reacted with some bands below 52 kDa; however, the extent of staining was very weak, especially in bands below 28 kDa.

Using the 24 human serum samples, changes in IgM antibody binding were examined on 1-D blots before and after treatment with NaOH. When 1-D blots treated with NaOH were used for testing, the same human sera were divided into three groups based on the degree of immunostaining of the 52-kDa band: (i) 11 sera showed almost unchanged antibody binding (Figure 2; strips 6, 8 and 10); (ii) three sera showed no antibody binding (Figure 2; strips 2 and 4); and (iii) 10 sera showed significantly reduced antibody binding, resulting in the formation of faint or thin bands (Figure 2; strips 12, 14 and 16).

Figure 1 Immunostaining of filaments (PTs) that extruded from *E. cuniculi*-germinated spores with human IgM antibodies or rabbit IgG antibodies. (a) Positive results obtained by a 1 : 200 dilution of H-168 human serum. Note the strongly positive signals on filaments that extruded from the germinated spores. (b) Positive results obtained by a 1 : 400 dilution from a symptomatic rabbit with natural *E. cuniculi* infection. Note the positive signals on the spore wall and the filament. Bars, 10 μm.

Culture supernatant containing MAb2 strongly reacted with a band at 52 kDa (Figure 2; strip P1). A serum from a naturally infected rabbit generated IgM antibody-positive multibands between 28 and 96 kDa, and also a few bands around 19 kDa (Figure 2; strip P2). However, the rabbit serum did not show any reduced influence in IgM antibody-binding of the 52-kDa band, even after NaOH treatment (Figure 2; strip P3).

Reactivities of ConA and mouse monoclonal antibody on 1-D blots before and after NaOH treatment

When untreated 1-D blots were used, ConA was the only one of seven lectins that revealed clearly positive binding to

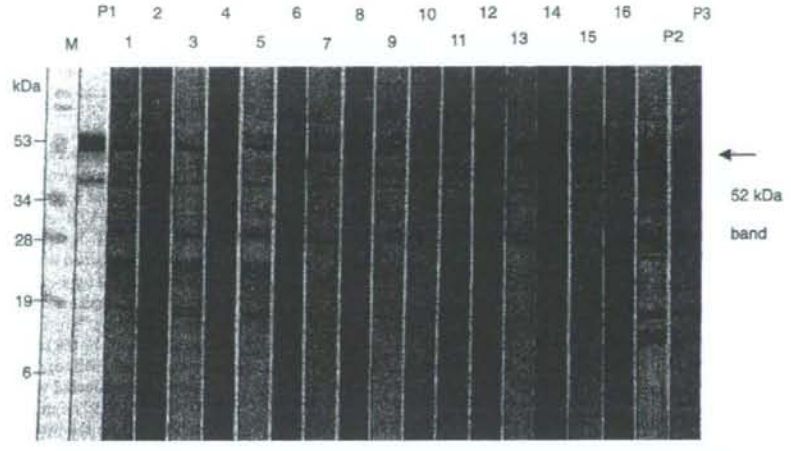

Figure 2 Binding profiles of human sera with anti-PT IgM antibody activities. *Encephalitozoon cuniculi* spore antigens were fractionated by 1-D PAGE and transferred to a PVDF membrane. Blotted strips before and after NaOH treatment were prepared and allowed to react with human serum samples followed by an anti-human IgM (μ-chain specific)-ALP conjugate. Odd-numbered strips and the P1- and P2-labelled strips were untreated, but even-numbered strips and the P3-labelled strip were treated with NaOH. Strips were reacted with each serum sample in pairs, starting from no. 1. M is a strip for markers of molecular weight (Prestained SDS-PAGE standards, Bio-Rad); P1 is a strip that reacted with MAb2; P2 and P3 are strips that reacted with a rabbit serum.

a 52-kDa band (data not shown). However, ConA did not bind at all to 1-D blots treated with NaOH (Figure 3; strip 2).

As seen on strip P1 in Figure 2 and strip 3 in Figure 3, MAb2 bound to the 52-kDa band on 1-D blots untreated with NaOH. However, MAb2-binding was not influenced by NaOH treatment at all (Figure 3; strip 4).

The location of the ConA-stained band on blotted strips was consistent with those bands detected by the monoclonal antibody (Figure 3). However, the band stained with ConA was always slightly thinner than bands detected by MAb2, suggesting that the PTP1 may be a mixture of different glycosylated and unglycosylated forms, which is likely to be slightly polydisperse in electrophoresis.

Identification of some proteins immunoreactive for human sera on 2-D blots

Eleven protein spots on a 2-D blot of *E. cuniculi* antigens were identified (Figure 4a, Table 1). Two of these spots, nos 1 and 2, had the same molecular size but different isoelectric points; these were identified as *E. cuniculi* polar tube protein (PTP), because both structures contained the peptide sequence ATALXSNAYGLTPGQQGMAQ by N-terminal amino acid sequencing. This has 90% sequence homology with the peptide sequence ATALCNAYGLTPGQQGMAQ of *E. cuniculi* genotype 1 (GenBank Accession No. AF310677) and was identified as PTP1 of *E. cuniculi* (SWISS-PRT

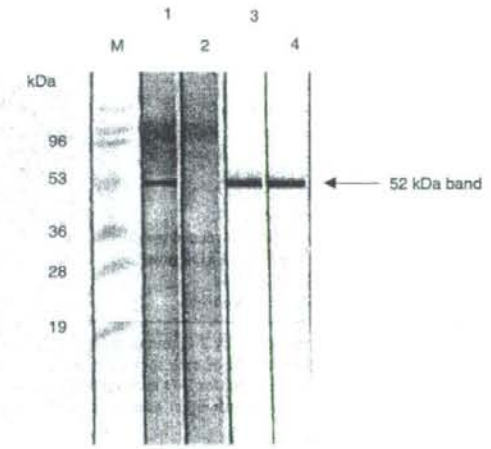

Figure 3 Binding profiles of ConA lectin and monoclonal antibody (MAb2) on 1-D blots. *Encephalitozoon cuniculi* spore antigens were fractionated by 1-D PAGE and transferred to a PVDF membrane. Blotted strips before and after NaOH treatment were prepared and allowed to react with ConA lectin and monoclonal antibody (MAb2). Odd-numbered strips were untreated, but even-numbered strips were treated with NaOH. Strip nos 1 and 2 and strip nos 3 and 4 were reacted with ConA and MAb2, respectively. M is a strip for markers of molecular weight (Prestained SDS-PAGE, Bio-Rad).

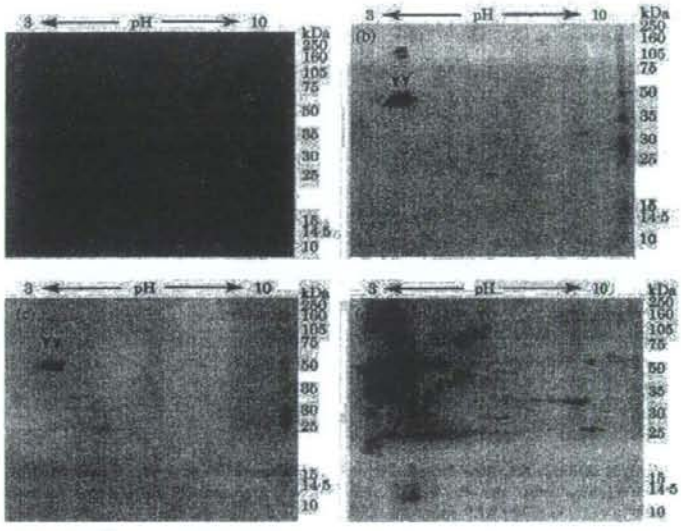

Figure 4 2-D immunoblot analysis. *Encephalitozoon cuniculi* spore antigens were fractionated by 2-D PAGE and transferred to PVDF membranes. (a) BODIPY FL-X staining: a blotted membrane is stained with the dye. Proteins extracted from 11 dye-stained spots (circles) identified by sequence analysis. (b–d) Immunostaining: blotted membranes incubated with H-168 serum (b), H-197 serum (c) and PRS (d). In the blotted membranes incubated with human sera (H-168 and H-197) containing anti-PT IgM antibodies, note the two acidic proteins (arrowheads) predominantly immunostained at 52 kDa; these proteins correspond to PTP1 spots capable of being stained with BODIPY FL-X, as seen in Figure 4(a).

Table 1 Human sera-immunoreactive spots in *E. cuniculi* identified by N-terminal amino acid sequencing (NTAAS) and LC-MS/MS

Spot no.	Protein	Accession no. (Swiss-Prot, NCBI)	Sequence coverage (%)	Method of identification	Immunoreactivity[a] with 168	197	PRS
1	Polar tube protein 1	sp. PTP1ENCCU	–	NTAAS	3+	3+	4+
2	Polar tube protein 1	sp. PTP1ENCCU	–	NTAAS	3+	3+	4+
3	Polar tube protein 2	gi: 19074274	21·3	LC-MS/MS	1+	0	2+
4	Translation elongation factor 1α	gi: 19074188	36·44	LC-MS/MS	0	0	1+
5	Spore wall protein 1	gi: 19074777	9·78	LC-MS/MS	0	0	2+
6	Hypothetical protein	gi: 19173268	42·86	LC-MS/MS	0	0	1+
7	Zinc finger protein	gi: 19074227	25·81	LC-MS/MS	1+	±	0
8	Similarity to HSP 70-related protein	gi: 19073931	29·55	LC-MS/MS	±	0	±
9	Heat shock-related 70 kDa protein	gi: 19173012	23·13	LC-MS/MS	0	0	±
10[b]	Phosphomannomutase	gi: 19173562	24·22	LC-MS/MS	0	0	0
11	6S proteasome ζ chain	gi: 19173680	17·67	LC-MS/MS	0	0	1+

[a]Immunoreactivity was examined by 2-D immunoblotting using human sera (H-168 and H-197) and rabbit sera (PRS – a pool of infected rabbit sera). The resultant intensity of each spot is scored as 0, ±, 1+, 2+, 3+ or 4+ (0, negative; ±, ambiguous; 1+ to 4+, graded positiveness). PRS was used as a positive control for 2-D immunoblot analysis.
[b]Spot no. 10 seems not to react with either human or rabbit samples, but was identified as a nonimmunogenic protein in this study.

database: PTP1ENCCU). This finding makes it clear that the 52-kDa PTP1 has more than one isoform.

H-168 and H-197 sera predominantly reacted with some spots that corresponded to PTP1 at 52 kDa (Figure 4b,c). These sera were examined as representative human sera with anti-PT IgM activities. H-168 serum also reacted with other protein spots, such as PTP2 and zinc finger protein (Figure 4b, Table 1). Such a positive reaction to zinc finger protein was not generated by a pool of sera from 11 naturally infected rabbits (PRS; Table 1).

When IgG antibodies in PRS were used as a positive control for 2-D immunoblot analysis, they reacted with spots that corresponded to PTP1, PTP2, spore wall protein 1, translation elongation factor 1α, hypothetical protein and 6S proteasome ζ chain in decreasing order of strength, as identified by LC-MS/MS analysis (Figure 4d, Table 1).

However, the rabbit IgG antibodies reacted very weakly with spots that corresponded to heat shock-related 70-kDa proteins (HSP70) and a protein with similarity to HSP70-related protein (Figure 4d, Table 1). Although a zinc finger protein and phosphomannomutase were also identified by LC-MS/MS analysis (Figure 4a), the corresponding spots were negative for rabbit IgG antibodies (Figure 4d, Table 1). IgG antibodies in a pool of 11 normal rabbit sera did not react with 2-D blots (data not shown).

Culture supernatant containing monoclonal antibody MAb2 reacted strongly with some spots of PTP1 at 52 kDa (data not shown).

DISCUSSION

All of the members of Microsporidia possess a unique, highly specialized structure, the PT, which is an organelle for invasion (15). *Encephalitozoon cuniculi* PT consists of three proteins: PTP1, PTP2 and PTP3 (16). The PTP1 is the major component of the PT and it is modified by O-linked mannose residues to which ConA binds (17).

In respect to antibodies against *Encephalitozoon* PT in immunocompetent persons, it has been reported that anti-*E. intestinalis* PT was demonstrated in 8% of Dutch blood donors and 5% of pregnant French women (18). Further study has demonstrated that carbohydrate moieties of the microsporidian PTPs are targeted by IgG in immunocompetent individuals (19). On the other hand, our study clearly indicates that the major activities of human anti-PT IgM antibodies are predominantly towards *E. cuniculi* PTP1, which is an acidic protein with an apparent molecular weight of 52 kDa in 2-D immunoblot analysis (Figure 4). Also, two chemically different antigenic sites can be found on the 52-kDa band in 1-D immunoblot analysis (Figure 2): proteinic determinant and saccharic determinant, as discussed below. In addition, although other few protein spots, such as PTP2 and zinc finger protein, weakly reacted with H-168 serum by 2-D immunoblotting, they did not appear to be effectively antigenic as compared to PTP1 (Table 1).

To analyse immunoreactivity of human anti-PT IgM with two different determinants, we used NaOH treatment capable of removing glycoepitopes from blotted antigens. Xu *et al.* (17) employed blots treated with 0·1 N NaOH at 50°C for 40 min to eliminate ConA binding to *E. hellem* PTP1. In our case, ConA binding to *E. cuniculi* PTP1 blotted onto a PVDF membrane was successfully eliminated by treating the blots with 0·05 M NaOH at 40°C for 16 h, conditions that were established by Duk *et al.* (13).

From the reactions of anti-PT IgM to the 52-kDa band after NaOH treatment, we could roughly group human sera into three categories when examined by 1-D immunoblotting: sera showing a completely negative profile; sera with a positive profile that was unmodified by NaOH treatment; and sera indicating a significantly reduced profile (Figure 2). Sera showing completely negative profiles are interpreted to have reacted with only a ConA-reactive determinant of PTP1 (Figure 2; strips 1–4). On the other hand, sera with a positive profile that was unmodified by NaOH treatment are interpreted to have reacted with only a proteinic determinant (Figure 2; strips 5–10). Interestingly, 41·3% (10/24) of the examined human serum samples belonged to the group with a significantly reduced profile. It was obvious that the significant reduction in binding after NaOH treatment resulted from the removal of the ConA-reactive determinant (Figure 2; strips 11–16), suggesting that this type of anti-PT IgM can recognize the saccharic determinant as well as the proteinic determinant. Thus, human anti-PT IgM could recognize the two determinants alone or in a pair, depending on serum used.

In a previous study (10) and also in this study, we confirmed that representative human sera with anti-PT IgM (H-168 and H-197) strongly immunostained the outer surface of filaments extruded from spores (Figure 1a). Our monoclonal antibody (MAb2) that could immunostain extruded PTs by ELISA definitely recognized the 52-kDa band by 1-D immunoblotting (Figures 2 and 3) and the PTP1 spots by 2-D immunoblotting (data not shown). Monoclonal and/or polyclonal antibodies raised to the purified *Encephalitozoon* PTP1 demonstrated reactivity with PTs by immunofluorescence and immunogold electron microscopy (17), indicating the presence of glycoconjugates in the PT. It has been proposed that the lipophilic regions of the PTPs adhere to the filament membrane and that the hydrophilic regions are orientated into the aqueous extrasporal environment (20). Thus, human anti-PT IgM-reactive determinants (constituted of saccharic and proteinic determinants and located on PTP1s) would be concentrated on the outside of the PTP coated on the surface of extruded filaments.

Regarding the specificity of anti-PT IgM in human sera, a previous study revealed that they did not react with extruded filaments from germinated *E. hellem* or *E. intestinalis*, indicating that human anti-PT IgM is species-specific (10). This finding was not in disagreement with previous findings that human sera containing anti-*E. intestinalis* PT IgG antibody activity did not immunostain filaments extruded from *E. cuniculi* or its PTP1 (19). One may consider that there is a cross-reactive relationship between microsporidian spores and fungal spores, because Microsporidia are phylogenetically related to fungi (21). However, apart from saccharic determinants, using an enzyme-linked immunosorbent assay, we found that MAb2 specific for *E. cuniculi* PTP1 did not cross-react with Laemmli sample buffer-extracted soluble antigens from the following fungi: *Candida albicans*, *Fusarium*

moniliforme, *Eurotium*, *Aspergillus fumigatus*, *Curvularis*, *Aureobasidium pullulans*, *Trichoderma* sp., *Chaetomium globosum* and *Rhizopus stolonifer* (data not shown).

In respect to the specific human immune responses to the *E. cuniculi* infection, anti-spore wall IgG was observed to precede anti-PT IgG (7). Strong antigenicity and immunogenicity of *E. cuniculi* PTP1 have also been reported (20). However, most of our subjects were negative for anti-spore wall IgM and IgG, as noted previously (10). Moreover, anti-PT IgG antibodies were not detectable in most of our subjects (10). Therefore, these subjects may have been exposed to *E. cuniculi* spores, but showed little secondary immune response to their exposure. There is still the possibility that such IgM antibodies are cross-reactive antibodies produced by fungal infections, since the primary response usually is of low specificity. In these regards, further work needs to be done.

Apart from some extremely rare situations, it is most unlikely that microsporidiosis is provoked by *E. cuniculi* in immunocompetent persons (2,4,8). Considering that almost all human encephalitozoonosis cases occurred in immunocompromised patients (2,4–6), one can speculate that protective immunity plays a very important role against *E. cuniculi* infection. We previously showed that the rate of positivity for anti-PT IgM antibodies was significantly higher among healthy people than among HIV-positive persons, such that the CD4 cell level greatly affected the detection of anti-PT IgM antibodies (10). It should be emphasized that human microsporidiosis is predominantly associated with $CD4^+$ T cell deficiency (8,22). A recent report on intraocular microsporidiosis in a patient with idiopathic $CD4^+$ T-lymphocytopenia proves the infectivity of *E. cuniculi* for immunodeficient humans (23).

In a model of PT discharge, it has been thought that unpolymerized PTP is released from the PT core and polymerizes on the outside of the membrane scaffolding as it is being everted (20). If circulating anti-PT IgM antibodies react with these unpolymerized and polymerized PTPs, resultant antigen–antibody complexes may block the formation of PTs, thus preventing the PT from penetrating a host cell. However, as in other human opportunistic protozoal infections, microsporidian-specific antibodies alone may not be protective (22). In humans, cell-mediated immunity is said to be critical for protection against microsporidian organisms (22). More recently, Sak *et al.* (24) demonstrated that humoral antibodies enhance the protective effect of $CD4^+$ T lymphocytes using SCID mice perorally infected with *E. cuniculi*, suggesting that the humoral part of the immune system may contribute to the defence against microsporidial infection. Further studies on human anti-PT IgM need to be performed from the perspective of protective immunity.

ACKNOWLEDGEMENTS

The authors appreciate the assistance of Shigeru Miwa (Immunobion, LTD., Sapporo, Japan) who contributed by producing the specific monoclonal antibody, MAb2. We also thank Tokiko Asakura for her assistance with the serological testing and cell culture.

This work was supported by Grant-in-Aid no. 16390177 from the Ministry of Education, Science, Sports and Culture of Japan.

REFERENCES

1 Canning EU & Varva J. Phylum Microsporidia. In Lee JJ, Leedale GF & Bradbury P (eds): *The Illustrated Guide to the Protozoa*, 2nd edn. Lawrence, KS, USA, Society of Protozoologists, 2000: 39–126.
2 Mathis A, Weber R & Deplazes P. Zoonotic potential of the Microsporidia. *Clin Microbiol Rev* 2005; **18**: 423–445.
3 Didier ES, Stovall ME, Green LC, Brindley PJ, Sestak K & Didier PJ. Epidemiology of microsporidiosis: sources and modes of transmission. *Vet Parasitol* 2004; **126**: 145–166.
4 Weber R, Schwartz DA & Deplazes P. Laboratory diagnosis of microsporidiosis. In Wittner M & Weiss LM (eds): *The Microsporidia and Microsporidiosis*. Washington, DC, ASM Press, 1999: 315–362.
5 Mohindra AR, Lee MW, Visvesvara G, *et al.* Disseminated microsporidiosis in a renal transplant recipient. *Transplant Infect Dis* 2002; **4**: 102–107.
6 Gamboa-Dominguez A, De Anda J, Donis J, Ruiz-Maza F, Visvesvara GS & Diliz H. Disseminated *Encephalitozoon cuniculi* infection in a Mexican kidney transplant recipient. *Transplantation* 2003; **75**: 1898–1900.
7 van Gool T, Biderre C, Delbac F, Wentink-Bonnema E, Peek R & Vivares CP. Serodiagnostic studies in an immunocompetent individual infected with *Encephalitozoon cuniculi*. *J Infect Dis* 2004; **189**: 2243–2249.
8 Bryan RT. Microsporidiosis as an AIDS-related opportunistic infection. *Clin Infect Dis* 1995; **21** (Suppl. 1): S62–S65.
9 Franzen C & Muller A. Microsporidiosis: human disease and diagnosis. *Microbes Infect* 2001; **3**: 389–400.
10 Omura M, Furuya K, Kudo S, Sugiura W & Azuma H. Detecting immunoglobulin M antibodies against microsporidian *Encephalitozoon cuniculi* polar tubes in sera from healthy and human immunodeficiency virus-infected persons in Japan. *Clin Vaccine Immunol* 2007; **14**: 168–172.
11 Asakura T, Nakamura S, Ohta M, Une Y & Furuya K. Genetically unique microsporidian *Encephalitozoon cuniculi* strain type III isolated from squirrel monkeys. *Parasitol Int* 2006; **55**: 159–162.
12 Galfre G, Howe SC, Milstein C, Butcher GW & Howard JC. Antibodies to major histocompatibility antigens produced by hybrid cell lines. *Nature* 1977; **266**: 550–552.
13 Duk M, Ugorski M & Lisowska E. β-elimination of *O*-glycans from glycoproteins transferred to immobilon P membranes: method and some applications. *Anal Biochem* 1997; **253**: 98–102.
14 Hellman U, Wernstedt C, Gonez J & Heldin CH. Improvement of an 'In-Gel' digestion procedure for the micropreparation of internal protein fragments for amino acid sequencing. *Anal Biochem* 1995; **224**: 451–455.

15 Xu Y & Weiss LM. The microsporidian polar tube: a highly specialized invasion organelle. *Int J Parasitol* 2005; **35**: 941–953.
16 Peuvel I, Peyret P, Metenier G, Vivares CP & Delbac F. The microsporidian polar tube: evidence for a third polar tube protein (PTP3) in *Encephalitozoon cuniculi*. *Mol Biochem Parasitol* 2002; **122**: 69–80.
17 Xu Y, Takvorian PM, Cali A, Orr G & Weiss LM. Glycosylation of the major polar tube protein of *Encephalitozoon hellem*, a microsporidian parasite that infects humans. *Infect Immun* 2004; **72**: 6341–6350.
18 van Gool T, Vetter JCM, Weinmayr B, Van Dam A, Derouin F & Dankert J. High seroprevalence of *Encephalitozoon* species in immunocompetent subjects. *J Infect Dis* 1997; **175**: 1020–1024.
19 Peek R, Delbac F, Speijer D, *et al*. Carbohydrate moieties of microsporidian polar tube proteins are targeted by immunoglobulin G in immunocompetent individuals. *Infect Immun* 2005; **73**: 7906–7913.
20 Keohane EM & Weiss LM. The structure, function, and composition of the microsporidian polar tube. In Wittner M & Weiss LM (eds): *The Microsporidia and Microsporidiosis*. Washington, DC, ASM Press, 1999: 196–224.
21 Thomarat F, Vivares CP & Gouy M. Phylogenetic analysis of the complete genome sequence of *Encephalitozoon cuniculi* supports the fungal origin of microsporidia and reveals a high frequency of fast-evolving genes. *J Mol Evol* 2004; **59**: 780–791.
22 Evering T & Weiss LM. The immunology of parasite infections in immunocompromised hosts. *Parasite Immunol* 2006; **28**: 549–565.
23 Kodjikian L, Garweg JG, Nguyen M, Schaffner T, Deplazes P & Zimmerli S. Intraocular microsporidiosis due to *Encephalitozoon cuniculi* in a patient with idiopathic CD4$^+$ T-lymphocytopenia. *Int J Med Microbiol* 2005; **294**: 529–533.
24 Sak B, Salat J, Horka H, Sakova K & Ditrich O. Antibodies enhance the protective effect of CD4$^+$ T lymphocytes in SCID mice perorally infected with *Encephalitozoon cuniculi*. *Parasite Immunol* 2006; **28**: 95–99.

MAJOR ARTICLE

Interleukin-4–Transgenic hu-PBL-SCID Mice: A Model for the Screening of Antiviral Drugs and Immunotherapeutic Agents against X4 HIV-1 Viruses

Kazu Okuma,[1] Reiko Tanaka,[1] Tomoyuki Ogura,[2] Mamoru Ito,[2] Sei Kumakura,[3] Mikiro Yanaka,[3] Masako Nishizawa,[4] Wataru Sugiura,[4] Naoki Yamamoto,[4] and Yuetsu Tanaka[1]

[1]Department of Immunology, Graduate School and Faculty of Medicine, University of the Ryukyus, Okinawa, [2]Central Institute for Experimental Animals, Kanagawa, and [3]Kureha Corporation and [4]National Institute of Infectious Diseases, Tokyo, Japan

CXCR4-tropic (X4) human immunodeficiency virus type 1 (HIV-1) does not efficiently infect and replicate in severe combined immunodeficiency (SCID) mice reconstituted with human peripheral blood mononuclear cells, termed "hu-PBL-SCID mice," due to, at least in part, relatively low levels of expression of the CXCR4 coreceptor. To overcome this limitation, interleukin (IL)–4–transgenic hu-PBL-SCID mice were derived that spontaneously synthesized human IL-4, which has been shown to enhance CXCR4 expression and promote X4 virus infection in vitro. Experiments reported here show that (1) synthesis of human IL-4 in vivo augmented CXCR4 expression on human CD4$^+$ lymphocytes and importantly led to productive infection of not only X4 HIV-1_{NL4-3} but also multidrug-resistant primary clinical isolates and that (2) the in vivo infection could be significantly blocked by the administration of a CXCR4 antagonist. Altogether, IL-4–transgenic hu-PBL-SCID mice provide a useful model for X4 HIV-1 study and testing/screening of anti-X4 viral drugs.

HIV-1 isolates enter target cells primarily after binding to the CD4 receptor and via the CXCR4 and CCR5 coreceptors [1–5] and are classified into X4 and R5 strains, respectively [6]. The X4 isolates are frequently implicated in the decline of peripheral CD4$^+$ T cell counts characteristic of the late stage of HIV-1 infection proceeding to the development of AIDS [7].

hu-PBL-SCID mice have been extensively used as a small animal model to study HIV-1 pathogenesis [8–14]. Results from a previous study showed that, although infection of human peripheral blood mononuclear cell (PBMC)–reconstituted hu-PBL-SCID mice with a predominantly R5 HIV-1 caused intensive CD4$^+$ T cell depletion, infection of similarly reconstituted mice with the same infectious dose of an X4 HIV-1 resulted in little or no CD4$^+$ T cell depletion [11]. Thereafter, it was noted that this limitation of X4 HIV-1 infection was due, at least in part, to a decrease in the intensity of CXCR4 expression on CD4$^+$ T cells [13]. Thus, it was reasoned that the pathogenic effects of the X4 HIV-1 strains in the hu-PBL-SCID mice might be related to the relative levels of the expression of HIV-1 coreceptor (the state of activation/differentiation) on human CD4$^+$ T cells at the time of infection in these mice. This limitation has to date restricted our ability to use this mouse model for understanding the mechanisms of X4 HIV-1 pathogenesis and for the evaluation of candidate therapeutics against X4 viruses. These findings prompted us to seek alternative strategies for the development of an improved hu-PBL-SCID mouse system that is permissive for infection/replication of X4 isolates.

Human interleukin (IL)–4 has been shown to specifically enhance the cell-surface expression of CXCR4 on

Received 1 May 2007; accepted 11 July 2007; electronically published 4 December 2007.

Potential conflicts of interest: none reported.

Presented in part: First International Workshop on Humanized Mice, Tokyo, 11–12 October 2006 (abstract P-15); 14th Conference on Retroviruses and Opportunistic Infections, Los Angeles, 25–28 February 2007 (abstract 496).

Financial support: Health and Labor Science Research Grant (Research on Publicly Essential Drugs and Medical Devices) from the Ministry of Health, Labor, and Welfare of Japan (grant H16-soyaku-004).

Reprints or correspondence: Dr. Kazu Okuma, Dept. of Immunology, Graduate School and Faculty of Medicine, University of the Ryukyus, Uehara 207, Nishihara-cho, Nakagami-gun, Okinawa 903-0215, Japan (kokuma@med.u-ryukyu.ac.jp).

The Journal of Infectious Diseases 2008; 197:134–41

0022-1899/2008/19701-0021$15.00
DOI: 10.1086/524303

resting peripheral blood T cells [15]. Furthermore, it has been reported that human IL-4 plays an important role in rendering $CD4^+$ T cells susceptible to X4 HIV-1 infection via enhanced cell-surface expression of the CXCR4 coreceptor in vitro [15–17].

In efforts to overcome the limitation inherent with the use of hu-PBL-SCID mice for the study of X4 HIV-1 as described above, we developed an IL-4–transgenic immunodeficient mouse model that consistently secreted readily detectable serum levels of human IL-4. We show here that X4 isolates readily infect/replicate in this mouse model but not in wild-type (wt) non–IL-4–transgenic mice and that this model can now be exploited for the rapid evaluation of the therapeutic efficacy of new anti-X4 HIV-1 agents in vivo.

METHODS

IL-4–producing mice. Two strains of human IL-4–transgenic immunodeficient mice were bred on the C.B-17-*scid* [18] and BALB/cA-Rag2$^{-/-}\gamma_c^{-/-}$ (dKO) genetic background mice [19, 20] at the Central Institute for Experimental Animals (CIEA) as follows. PBMCs were isolated from a healthy human volunteer and activated in vitro with pokeweed mitogen. RNA was prepared from these PBMCs, and then cDNA was synthesized by reverse-transcriptase polymerase chain reaction (PCR). Human IL-4 cDNA was amplified from the cDNA using one set of primers: 5'-CCCGGGATCGTTAGCTTCTCCTGATAAAA-3' and 5'-GCGGCCGCTATTCAGCTCGAACACTTTGAAT-3'. The product was inserted into the PCR2.1 vector by use of the TA cloning kit (Invitrogen) and the insert sequenced. After confirmation of the sequence, IL-4 cDNA was inserted into pCMVb with a CMV promoter (Invitrogen). To produce transgenic mice, a DNA fragment containing the CMV promoter, IL-4 cDNA, and Poly(A) regions was excised with *Xho*I and *Hind*III sites of pCMVb and microinjected into the pronuclei of fertilized eggs from the 2 strains (C.B-17-*scid* and BALB/cA-dKO) of mice. These eggs were subsequently transplanted into oviducts of pseudopregnant foster recipient mice. The offspring mice were screened to confirm the insertion of the transgene into the genome by PCR, and serum from these mice was screened for levels of human IL-4 by ELISA with a commercial kit (BD). The IL-4 transgene–hemizygous mice were maintained by mating them with wt mice with the same genetic background in the specific-pathogen-free (SPF) facility of the CIEA. The mice were transferred to the SPF and biosafety level 3 facilities of the Institute for Animal Experiments, University of the Ryukyus, and were used for further experiments. The experimental protocols were approved by the Institutional Animal Care and Use Committee on the basis of the Regulation for Animal Experimentation of the CIEA and University of the Ryukyus before the initiation of the study.

Viruses. X4 HIV-1_{NL4-3} was obtained as described elsewhere [14]. Fourteen multidrug-resistant (MDR) HIV-1 clinical isolates were obtained from HIV-1–infected patients who had been treated with highly active antiretroviral therapy (HAART). The viruses were propagated in PBMCs stimulated with phytohemagglutinin (PHA; Sigma), IL-2 (National Institutes of Health AIDS Research and Reference Reagent Program), and IL-4 (Peprotec). Three isolates from these MDR isolates that efficiently grew in the activated cells were selected for further experiments. The titers of virus stocks were determined by end-point titration using a 2-fold limiting dilution of the stock and in vitro PHA-activated human PBMCs, and the infectious units (IU) were calculated.

CXCR4 antagonist. The synthesis and purification of the CXCR4 antagonist KRH-1636 were performed at Kureha Corporation as described elsewhere [21]. As a control, the carrier tartrate was used in parallel.

Transplantation and infection. The control (wt) and the IL-4–transgenic C.B-17-*scid* mice were depleted of NK cells by the intraperitoneal (ip) injection of 0.5–1.0 mg of anti–mouse IL-2R β (TMβ-1) [22] per animal. The IL-4–transgenic and the control BALB/cA-dKO mice do not require TMβ-1 treatment because they lack NK cells [19, 20]. PBMCs were isolated from healthy human donors. Groups of 2–4-month-old IL-4–transgenic mice from each of the 2 background strains and their corresponding non–IL-4–transgenic wt mice were injected ip with PBMCs 3 days later. Groups of mice were challenged 24 h later ip with mock, HIV-1_{NL4-3}, or MDR isolates (2000 IU/500 μL/animal). For the experiments using the CXCR4 antagonist, groups of mice were administered 0.1 mL of 10 mmol/L KRH-1636, the tartrate carrier or saline ip at 1 h before and 1 day after virus infection. At 6–8 days after infection, the mice were killed, their blood was obtained by cardiocentesis, and human lymphocytes were collected from the peritoneal lavage fluids. The serum samples were assayed for levels of human IL-4 by use of an ELISA kit (R&D Systems). The human lymphocytes were analyzed using flow cytometry as described below. The remaining cells were cultured in RPMI 1640 medium (Sigma) supplemented with fetal calf serum and IL-2. The peritoneal lavage fluids, serum samples, and lymphocyte culture supernatants were examined for levels of p24 by use of an ELISA kit (Zepto Metrix).

Flow cytometry analysis. Cell samples to be analyzed by flow cytometry were initially incubated with normal human IgG for blocking of the Fc receptors. For cell-surface staining, aliquots of cells were then stained with Cy5-labeled anti-CD4 (OKT4) and phycoerythrin-labeled anti-CXCR4 (12G5; Dako) or with Cy5-labeled anti-CD3 (OKT3). For intracellular staining, after CD3 staining the aliquots of cells were fixed, permeabilized, and incubated with fluorescein isothiocyanate–labeled anti–HIV-1 Gag p24 (2C2; Y.T. et al., unpublished data). Stained samples were analyzed on a FACSCalibur flow cytometer, using Cell Quest software (BD Pharmingen). Aliquots of cells stained

Table 1. Expression of human CD4, CXCR4, and intracellular HIV-1 p24 in cells from X4 HIV-1–infected hu-PBL-SCID mice.

Category	X4 HIV-1 infection	Mice, no.	$CD4^+$ T cells, %	*P*	$CXCR4^+CD4^+$ T cells, %	*P*	$p24^+$ T cells, %	*P*
C.B-17-*scid* mice								
Control	NL4-3	6	22.1 ± 8.3	<.001	45.2 ± 4.7	<.001	0.1 ± 0.1	NS
IL-4 transgenic	NL4-3	6	66.3 ± 9.0		85.5 ± 6.1		0.1 ± 0.1	
BALB/cA-dKO mice								
Control	NL4-3	5	35.9 ± 5.1	<.01	92.6 ± 1.4	<.001	0.2 ± 0.1	<.05
IL-4 transgenic	NL4-3	3	57.4 ± 8.3		68.2 ± 3.9		3.2 ± 1.2	

NOTE. Cells in peritoneal lavage fluid from control and interleukin (IL)–4–transgenic hu-PBL-SCID mice on either the C.B-17-*scid* or BALB/cA-dKO background were labeled with appropriate monoclonal antibodies and analyzed by flow cytometry, as described in Methods. Analyzed data are shown as mean ± SD values. NS, not significant. The indicated *P* values for the comparison of control vs. transgenic mice for each category are based on Student's *t* test.

with or without each of the antibodies described above were used as controls for the purposes of establishing gates and for the determination of the frequency of positive cells.

Statistical analysis. Data obtained by flow cytometry were analyzed by Student's *t* test with GraphPad Prism (version 4.0c for Mac OS X; GraphPad Software).

RESULTS

Production of human IL-4 in IL-4–transgenic mice. Efforts to construct the IL-4–transgenic mice constitutively synthesizing human IL-4 finally led to the establishment of mice on each of the 2 immunodeficient backgrounds expressing either high or low serum levels of human IL-4 (data not shown). On the basis of preliminary data obtained on the efficiency of virus replication, all subsequent experiments were done using only the 2 strains with high serum IL-4 expression levels. We assayed for levels of human IL-4 in the serum from the $IL\text{-}4^+$ hu-PBL-SCID mice and the wt hu-PBL-SCID mice on either the C.B-17-*scid* or BALB/cA-dKO background after infection with X4 HIV-$1_{NL4\text{-}3}$. Serum from each of the IL-4–transgenic mice on either background contained significant levels of human IL-4 (~800–1800 pg/mL), whereas serum from the control mice on the same background showed nondetectable levels of human IL-4. These data demonstrate that the human IL-4 synthesized by the IL-4–transgenic mice is generated from the transgene but not from the human PBMCs transplanted in these mice.

Effect of human IL-4 on the levels of human CXCR4 and CD4 expression by cells transplanted into mice. Since human IL-4 has been previously documented to enhance the expression of CXCR4 in vitro, experiments were done to examine the expression of human CXCR4 on transplanted $CD4^+$ cells in the peritoneal lavage fluids from HIV-$1_{NL4\text{-}3}$–infected $IL\text{-}4^+$ hu-PBL-SCID mice and control hu-PBL-SCID mice on either the C.B-17-*scid* or BALB/cA-dKO background. There did not appear to be any detectable difference in the absolute amounts of cells recovered from the peritoneal lavage fluids from the IL-4–positive or IL-4–negative hu-PBL-SCID mice on either background (data not shown). Flow cytometry analysis demonstrated that the frequency of human $CD4^+$ cells from the IL-4–transgenic C.B-17-*scid* or BALB/cA-dKO mice was significantly higher than that from the control mice (table 1). As expected, there was a marked increase in the frequency of CXCR4-expressing $CD4^+$ cells from the IL-4–transgenic mice on either genetic background relative to that from the control mice (figure 1*A* and table 1). Thus, these data indicate that human IL-4 produced endogenously is functional in vivo in terms of its ability to enhance human CXCR4 expression on $CD4^+$ cells transplanted into the mice.

Increased frequency of X4 HIV-1–infected cells from IL-4–transgenic hu-PBL-SCID mice. Since the constitutive synthesis of human IL-4 in IL-4–transgenic hu-PBL-SCID mice resulted in the enhanced expression of X4 HIV-1 receptors (human CXCR4/CD4) on the transplanted cells, we reasoned that such cells were likely to be more permissive to the infection and replication of X4 HIV-1. We thus challenged the IL-4–transgenic hu-PBL-SCID mice and control hu-PBL-SCID mice bred on the C.B-17-*scid* or BALB/cA-dKO mice with HIV-$1_{NL4\text{-}3}$. Cells obtained from the peritoneal lavage fluids were analyzed for cell-surface expression of human CD3 (since HIV-1 downmodulates CD4 expression) and the presence of intracellular p24. As seen in figure 1*B* and table 1, although very few if any $CD3^+$ cells from the control or IL-4–transgenic C.B-17-*scid* mice showed p24 expression, there was a >10-fold increase in the frequency of $CD3^+$ T cells that expressed p24 from the IL-4–transgenic BALB/cA-dKO mice relative to the control mice. These data suggest that, while transgene-induced human IL-4 increases the frequency of $CD4^+CXCR4^+$ T cells transplanted into both the C.B-17-*scid* and the BALB/cA-dKO mice, only the latter demonstrates increased sensitivity to X4 HIV-1 infection and replication, at least when this assay is used (see below).

High production of X4 HIV-1 in the culture supernatants of cells from IL-4–transgenic hu-PBL-SCID mice. In an effort

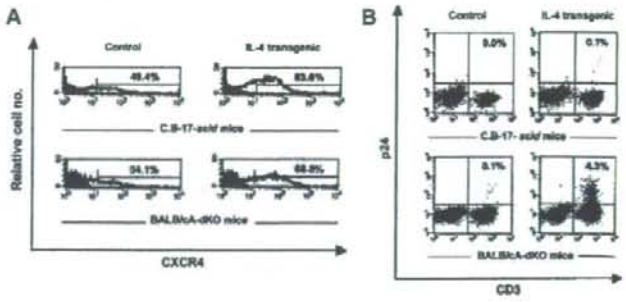

Figure 1. Enhancement of the expression of CXCR4 coreceptor and facilitation of X4 HIV-1 infection and replication in hu-PBL-SCID mice by in vivo production of human interleukin (IL)–4. Groups of hu-PBL-SCID mice, generated from IL-4–transgenic and nontransgenic (control) mice on either the C.B-17-*scid* or BALB/cA-dKO background, were injected intraperitoneally with HIV-1_{NL4-3} at −24 h after peripheral blood mononuclear cell (PBMC) reconstitution. Six to eight days later, peritoneal lavage fluids were harvested from mice in each group, and cells were collected from the fluids by density-gradient centrifugation. *A*, Cells analyzed for the frequency and mean density of human CXCR4 expression on CD4+ cells by flow cytometry. Data for analyzed cells are depicted by a thick line, and the background control profile is depicted by a thin line and gray shading. The nos. above the bars represent the percentage of positive cells. Data shown are representative of mice in each group from 3 independent experiments. *B*, HIV-1 infectivity. Cells were subjected to flow cytometry after cell-surface CD3 and intracellular p24 staining. Analyzed data are depicted as dot plots. The nos. in the graphs indicate the percentage of CD3+p24+ cells. Data displayed are representative of mice in each group from 3 independent experiments.

to determine the reason for our failure to detect levels of intracellular p24 in the IL-4–transgenic mice on the C.B-17-*scid* background and to further support the above finding, peritoneal lavage fluids were collected from mock- or HIV-1_{NL4-3}–infected IL-4+ hu-PBL-SCID mice and, for purposes of control, the HIV-1_{NL4-3}–infected non–IL-4–transgenic mice on the C.B-17-*scid* background. The cells were isolated from the peritoneal lavage fluids, and an aliquot was analyzed for the frequency and the relative density of human CXCR4/CD4; the remaining aliquot was cultured in vitro. In addition, the peritoneal lavage fluids and the culture supernatants of cells at days 1–3 after culture were assayed for levels of p24 production. As displayed in table 2, although the frequency of CXCR4+CD4+ cells in the IL-4–transgenic mice was significantly higher than that in the nontransgenic mice, the mean fluorescence intensity (MFI) of CXCR4 expressed by the CD4+ T cells from these mice was not increased compared with the control (because of an increase in the frequency of CXCR4+CD4+ cells with relatively low MFI; see figure 1*A*). Analysis of levels of synthesized p24 demonstrated marked differences, as shown in figure 2. Thus, although the amounts of p24 produced were modest in the peritoneal lavage fluids and the cell-culture supernatants from HIV-1–infected control mice, the levels of p24 produced by those from HIV-1–infected IL-4–transgenic mice were strikingly higher (15,429, 11,844, 1696, and 53 pg/mL in the supernatants on day 3) (mean, 48.9 vs. 7255 pg/mL; >100-fold increase). Although the levels of p24 produced by one of the IL-4–transgenic mice (mouse 12) were similar to those in the control mice, this was likely due to the much lower relative level of human IL-4 (354 pg/mL in serum) produced by mouse 12 than those from the other 3 IL-4–transgenic mice (4227, 6313, and 2356 pg/mL in serum). The present data not only document the fact that the cells from these

Table 2. Effect of the CXCR4 antagonist KRH-1636 on the expression of human CXCR4 by CD4+ cells from X4 HIV-1–infected interleukin (IL)–4–transgenic hu-PBL-SCID mice.

C.B-17-*scid* mice	X4 HIV-1 infection	CXCR4 antagonist	Mice, no.	CXCR4+CD4+ T cells, %	*P*	CXCR4 on CD4+ T cells, MFI	*P*
Control	NL4-3	Mock	4	45.5 ± 9.3	<.05[a]	78.7 ± 36.0	NS[a]
IL-4 transgenic	NL4-3	Mock	4	66.7 ± 7.4	NS[b]	73.1 ± 6.2	<.05[b]
IL-4 transgenic	NL4-3	KRH-1636	4	63.0 ± 4.2		62.2 ± 4.6	

NOTE. Control or IL-4–transgenic hu-PBL-SCID mice on the C.B-17-*scid* background infected with X4 HIV-1_{NL4-3} were administered mock KRH-1636 or real KRH-1636. Cells isolated from the peritoneal lavage fluid from the mice in each group were labeled with appropriate monoclonal antibodies and subjected to flow cytometry, as described in Methods. Data analyzed are displayed as mean ± SD values. MFI, mean fluorescence intensity; NS, not significant. The indicated *P* values are based on Student's *t* test.

[a] For the comparison between control mice and IL-4–transgenic mice that received a mock CXCR4 antagonist.

[b] For the comparison between IL-4–transgenic mice that received a mock CXCR4 antagonist and IL-4–transgenic mice that received KRH-1636.

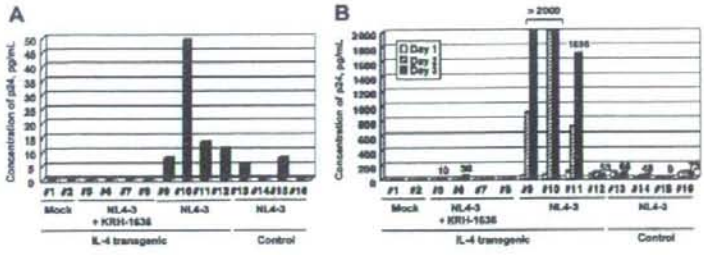

Figure 2. Efficient infection of interleukin (IL)–4–producing hu-PBL-SCID mice with X4 laboratory strain and an inhibitory effect of the CXCR4 antagonist KRH-1636 on infection. Twelve IL-4–transgenic and 4 nontransgenic (control) hu-PBL-SCID mice were generated on the C.B-17-*scid* background. Among them, 8 IL-4–transgenic and 4 control mice were infected intraperitoneally (ip) with the X4 laboratory strain (HIV-1_{NL4-3}) and 4 IL-4–transgenic mice were mock-infected at 1 day after engraftment. To evaluate the effect of KRH-1636, this drug was administered ip twice, at 1 h before and 1 day after infection of 4 IL-4–transgenic mice (NL4-3 + KRH-1636). At 8 days after infection, peritoneal lavage fluids were obtained from the mice in each group. Cells were isolated from the fluids and cultured in IL-2–containing medium. Levels of HIV-1 p24 in the peritoneal lavage fluids *(A)* and culture supernatants at days 1–3 after incubation *(B)* were quantitated for infectivity and replication efficiency by ELISA. With regard to the data on mock-infected mice, only 2 of 4 representative data are presented. The nos. listed above the bars in the graph indicate levels of HIV-1 p24 when it was detectable on day 3 (most of the values were <200 pg/mL, and select samples showed values of >2000 pg/mL). Pound signs (#) indicate mouse nos. Results shown are representative of 3 independent experiments.

IL-4–transgenic C.B-17-*scid* mice are susceptible but also demonstrate that the virus from such cells is replication competent. In addition, these findings suggest that the use of intracellular p24 levels is not a sensitive enough technique and that data using the intracellular p24 assay need to be carefully evaluated. These data also indicate that the IL-4–transgenic hu-PBL-SCID mice provide a powerful model for the study of X4 HIV-1 infection independently of the genetic background of the mice.

Inhibitory effect of the CXCR4 antagonist on infection of IL-4–transgenic hu-PBL-SCID mice with the X4 laboratory strain. In an effort to further validate that the CXCR4 coreceptor was indeed used by the X4 HIV-1 virus in the IL-4–transgenic hu-PBL-SCID mice, we used the X4 virus-entry inhibitor, CXCR4 antagonist KRH-1636. Thus, the IL-4–transgenic hu-PBL-SCID mice on the C.B-17-*scid* background were infected with X4 laboratory strain HIV-1_{NL4-3} and were either mock treated or treated with KRH-1636, and the peritoneal lavage fluids, cells in fluids, and cell-culture supernatants were examined as described above. As shown in table 2, the frequency of $CXCR4^+CD4^+$ cells in KRH-1636–treated IL-4–transgenic mice was marginally lower than that in mock-treated IL-4–transgenic mice. In addition, the MFI of CXCR4 expression by the $CD4^+$ T cells was clearly reduced by KRH-1636 administration. Importantly, treatment with KRH-1636 almost completely blocked X4 HIV-1 infection in these IL-4–transgenic mice (figure 2). These data indicate that X4 HIV-1 infection in transgenic mice is CXCR4 dependent and that our mouse model can be used to develop and test new anti-X4 HIV-1 drugs in vivo.

Therapeutic effect of KRH-1636 on the infection of IL-4–transgenic hu-PBL-SCID mice with MDR clinical isolates. The appearance of MDR HIV-1 clinical isolates has been and continues to be one of the growing problems in a significant number of patients receiving HAART and seriously limits the use of the antiviral drugs that are currently available. Thus, the development of novel adjunct or alternative therapeutics is an urgent need. Since treated patients tend to harbor significantly higher levels of either dual/mixed or X4 viruses [23] and since MDR isolates are not usually refractory to new treatment with drugs from classes that have not been used previously in patients from which the viruses were derived, we finally wanted to examine the effect of KRH-1636 on MDR HIV-1 infection in IL-4–transgenic hu-PBL-SCID mice. For this experiment, we used the IL-4–transgenic BALB/cA-dKO mice instead of the IL-4–transgenic C.B-17-*scid* mice, because the former seems more permissive to X4 HIV-1 infection than the latter, as described above. Before the in vivo study, we confirmed that the in vitro infection by 3 MDR clinical isolates could be inhibited with KRH-1636 (more than ~90% inhibition at the 5-μmol/L level). Thus, groups of IL-4–transgenic hu-PBL-SCID mice were infected with a mixture of these selected MDR isolates containing equal IU of each virus and treated with KRH-1636 or the tartrate carrier control. Thereafter, the cells obtained from the peritoneal lavage fluids were analyzed for the expression of cell-surface human CD4, CD3, and intracellular p24. The serum, peritoneal lavage fluids, and supernatants following in vitro culture of the cells for 24 h were assayed for levels of p24 production. Flow cytometry analysis after CD4 staining demonstrated a significant decline in $CD4^+$ T cells in 2 (mouse 7 and mouse 8) of 4 control-treated mice (figure 3*A*; top profile shows data from 1 of these 2 mice), which was likely due to MDR HIV-1 pathogenesis. However, importantly, no detectable depletion of $CD4^+$ T cells was observed in any of 4 KRH-1636–treated mice (figure 3*A*; bottom profile). As summarized in table 3, the difference in the frequency of $CD4^+$ T cells between the control-treated mice and the

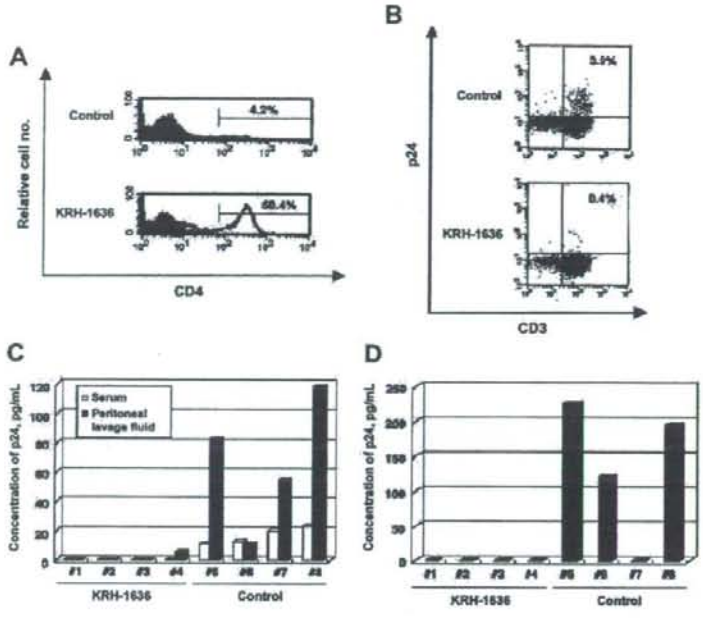

Figure 3. Prophylactic effect of KRH-1636 on infection and pathogenesis by multidrug-resistant (MDR) HIV-1 clinical isolates. Eight interleukin (IL)–4–transgenic hu-PBL-SCID mice (BALB/cA-dKO) were infected intraperitoneally (ip) with a mixture of MDR HIV-1 clinical isolates at 1 day after human peripheral blood mononuclear cell transfer. In an effort to assess the effect of KRH-1636 on HIV-1 infection, this agent or tartrate (control drug) was administered to 4 mice per group ip twice, at 1 h before infection and 1 day after infection. At 7 days after infection, serum and peritoneal lavage fluids were harvested from mice in each group, and cells were collected from the fluids. *A*, Cells examined for human CD4 expression by cell-surface staining and standard flow cytometry. Representative data from a single mouse from the control-treated or the KRH-1636–treated HIV-1–infected mice are shown. The frequency of $CD4^+$ T cells is depicted by a thick line, and the background control is depicted by a thin line with gray shading. The nos. above the bars indicate the percentage of positive cells. *B*, Aliquot of the peritoneal lavage cells analyzed by flow cytometry for the frequency of $CD3^+$ T cells that were positive for the intracellular presence of HIV-1 p24. Representative data of cells from the control-treated and the KRH-1636–treated HIV-1–infected mice are shown. The nos. in the graphs indicate the percentage of $CD3^+p24^+$ cells. *C*, Concentrations of p24 in serum and peritoneal lavage fluid. Concentrations were determined by ELISA to quantify MDR HIV-1 infection and replication efficiency. Pound signs (#) indicate mouse nos. *D*, Levels of in vitro p24 production. The remaining cells were cultured in a microtiter plate containing IL-2^+ medium for ~24 h, and the culture supernatants obtained were assayed for levels of in vitro p24 production by ELISA. Pound signs (#) indicate mouse nos. Results shown are representative of 3 similar independent experiments.

KRH-1636–treated mice was not significant. However, the MFI of CD4 expression was significantly decreased in the control-treated mice (229.3 vs. 296.3; $P < .05$). Results of CD3/p24 staining showed that the frequency of $CD3^+p24^+$ cells was markedly inhibited in the KRH-1636–treated mice, compared with that in the carrier-treated control mice (figure 3*B* and table 3). Furthermore, levels of HIV-1 p24 in the serum samples, peritoneal lavage fluids, and culture supernatants from the KRH-

Table 3. Effect of KRH-1636 on infection and pathogenesis by multidrug-resistant (MDR) HIV-1 clinical isolates in interleukin (IL)–4–transgenic hu-PBL-SCID mice.

BALB/cA-dKO mice	X4 HIV-1 infection	CXCR4 antagonist	Mice, no.	$CD4^+$ T cells, %	*P*	$CD4^+$ T cells, MFI	*P*	$p24^+$ T cells, %	*P*
IL-4 transgenic	MDR	Control	4	14.7 ± 11.9	NS	229.3 ± 33.0	< .05	8.2 ± 0.8	< .01
IL-4 transgenic	MDR	KRH-1636	4	31.3 ± 15.7		296.3 ± 25.2		0.8 ± 0.7	

NOTE. IL-4–transgenic hu-PBL-SCID mice on the BALB/cA-dKO background were infected with MDR HIV-1 clinical isolates and administered tartrate (control) or KRH-1636. Cells in peritoneal lavage fluid from the mice in each group were stained with appropriate monoclonal antibodies and analyzed by flow cytometry, as described in Methods. Data shown here are mean ± SD values. MFI, mean fluorescence intensity; NS, not significant. The indicated *P* values for the comparison between control mice and mice that received KRH-1636 are based on Student's *t* test.

1636–treated HIV-1–infected mice were almost completely reduced relative to those in the control mice (figure 3*C* and 3*D*). Note that the failure to detect the in vitro production of p24 in mouse 7 might result from depletion of $CD4^+$ T cells (figure 3*D*). These data demonstrate that the CXCR4 antagonist KRH-1636 has a marked degree of prophylactic effect on infection with pathogenic MDR clinical isolates in vivo.

DISCUSSION

Humanized mice that have served as valuable small animal models include the SCID-hu Thy/Liv mouse [24–28]. This mouse model, generated by implanting human hematopoietic tissues (human fetal thymus/liver) under the kidney capsule, has been used for the study of HIV-1 and is known for permissiveness to X4 HIV-1 infection [26–28]. However, the use of this model is limited by the fact that the implants are of human fetal organ origins that are not easily available. On the other hand, the hu-PBL-SCID mouse model provides another surrogate in vivo HIV-1 infection assay system. Although this model has led to a number of successful studies of HIV-1 [8–14], there was still a limitation in that it was difficult to demonstrate X4 HIV-1 infection and replication in such mice. Thus, to add extra value to the use of this mouse system for the study of HIV-1, in the present study we developed novel human IL-4–transgenic hu-PBL-SCID mice that enable CXCR4-using HIV-1 strains to efficiently infect and replicate in these mice.

Human IL-4 has low homology with murine IL-4 both at the gene and protein levels, accounting for the lack of cross-reactivity of this cytokine in the 2 species in vitro [29–32]. Results of the experiments reported here indicate that the high efficiency of X4 HIV-1 infection in the IL-4–transgenic hu-PBL-SCID mice was, at least in part, secondary to enhanced expression of viral receptors induced by human IL-4 synthesized endogenously. Interestingly, although there was no apparent increase in the number of cells recovered from the engrafted transgenic mice, there was a significant increase in the number of $CD4^+$ T cells recovered (1.5–3-fold). It is thus possible that the other cell lineages migrate from the peritoneal cavity to other tissues of the mice, resulting in enrichment of the $CD4^+$ T cell lineage. However, further studies of other tissues are needed to clarify this issue. Furthermore, our preliminary experiments indicate that the IL-4–transgenic hu-PBL-SCID mice remain permissive to R5 strain infection (data not shown).

In this report, we created 2 types of novel hu-PBL-SCID mice by transplanting human PBMCs into IL-4–transgenic C.B-17-*scid* and BALB/cA-dKO mice. The data obtained show that hu-PBL-SCID mice using the IL-4–producing BALB/cA-dKO mice appeared more permissive to X4 HIV-1 infection than did those using the IL-4–producing C.B-17-*scid* mice, at least as determined by the presence of intracellular p24. Although the reasons for this difference remain to be determined, it should be noted that, whereas the BALB/cA-dKO mice were derived by double mutation with defects in both the recombinase-activating gene 2 (Rag-2) and the gene encoding the γ_c chain of select cytokine receptors [19, 20], the C.B-17-*scid* mice have only the Rag-2 mutation [18]. Thus, although the Rag-2 mutation prevents the normal maturation of T and B lymphocytes, the γ_c chain mutation abrogates the expression of functional receptors for IL-2 and other cytokines, preventing the expansion of lymphocytes, including NK cells, which play an important role in the innate immune response such as nonspecific rejection of xenogeneic grafts. It is thus possible that the C.B-17-*scid* mice maintain a low but significant residual level of NK cell function, which may play a role in the difference noted above even though they were administered significant levels of anti–IL-2Rβ antibody. Since the BALB/cA-dKO mice are completely deficient in NK cell lineage and function, they are more immunodeficient than the C.B-17-*scid* mice, suggesting that the level and type of immunodeficiency in the BALB/cA-dKO mice may facilitate better engraftment and more efficient viral infection and propagation within these mice. These select defects of the BALB/cA-dKO mice might render the IL-4–transgenic mouse model on this background more valuable and ideal for studies of X4 HIV-1.

Acknowledgments

We thank the National Institutes of Health AIDS Research and Reference Reagent Program and M. Sasaki for supplying interleukin-2 and technical support, respectively. We are also grateful to Prof. Aftab Ansari for his critical reading of the manuscript and for his helpful discussion about and suggestions for the manuscript.

References

1. Feng Y, Broder CC, Kennedy PE, Berger EA. HIV-1 entry cofactor: functional cDNA cloning of a seven-transmembrane, G protein-coupled receptor. Science **1996**; 272:872–7.
2. Alkhatib G, Combadiere C, Broder CC, et al. CC CKR5: a RANTES, MIP-1alpha, MIP-1beta receptor as a fusion cofactor for macrophage-tropic HIV-1. Science **1996**; 272:1955–8.
3. Berson JF, Long D, Doranz BJ, Rucker J, Jirik FR, Doms RW. A seven-transmembrane domain receptor involved in fusion and entry of T-cell-tropic human immunodeficiency virus type 1 strains. J Virol **1996**; 70: 6288–95.
4. Deng H, Liu R, Ellmeier W, et al. Identification of a major co-receptor for primary isolates of HIV-1. Nature **1996**; 381:661–6.
5. Doranz BJ, Rucker J, Yi Y, et al. A dual-tropic primary HIV-1 isolate that uses fusin and the beta-chemokine receptors CKR-5, CKR-3, and CKR-2b as fusion cofactors. Cell **1996**; 85:1149–58.
6. Berger EA, Doms RW, Fenyo EM, et al. A new classification for HIV-1. Nature **1998**; 391:240.
7. Xiao L, Rudolph DL, Owen SM, Spira TJ, Lal RB. Adaptation to promiscuous usage of CC and CXC-chemokine coreceptors in vivo correlates with HIV-1 disease progression. AIDS **1998**; 12:F137–43.
8. Mosier DE. Adoptive transfer of human lymphoid cells to severely immunodeficient mice: models for normal human immune function, autoimmunity, lymphomagenesis, and AIDS. Adv Immunol **1991**; 50:303–25.
9. Mosier DE, Gulizia RJ, Baird SM, Wilson DB, Spector DH, Spector SA. Human immunodeficiency virus infection of human-PBL-SCID mice. Science **1991**; 251:791–4.

10. Torbett BE, Picchio G, Mosier DE. hu-PBL-SCID mice: a model for human immune function, AIDS, and lymphomagenesis. Immunol Rev 1991; 124:139–64.
11. Mosier DE, Gulizia RJ, MacIsaac PD, Torbett BE, Levy JA. Rapid loss of CD4+ T cells in human-PBL-SCID mice by noncytopathic HIV isolates. Science 1993; 260:689–92.
12. Rizza P, Santini SM, Logozzi MA, et al. T-cell dysfunctions in hu-PBL-SCID mice infected with human immunodeficiency virus (HIV) shortly after reconstitution: in vivo effects of HIV on highly activated human immune cells. J Virol 1996; 70:7958–64.
13. Fais S, Lapenta C, Santini SM, et al. Human immunodeficiency virus type 1 strains R5 and X4 induce different pathogenic effects in hu-PBL-SCID mice, depending on the state of activation/differentiation of human target cells at the time of primary infection. J Virol 1999; 73:6453–9.
14. Yoshida A, Tanaka R, Murakami T, et al. Induction of protective immune responses against R5 human immunodeficiency virus type 1 (HIV-1) infection in hu-PBL-SCID mice by intrasplenic immunization with HIV-1-pulsed dendritic cells: possible involvement of a novel factor of human CD4+ T-cell origin. J Virol 2003; 77:8719–28.
15. Jourdan P, Abbal C, Noraz N, et al. IL-4 induces functional cell-surface expression of CXCR4 on human T cells. J Immunol 1998; 160:4153–7.
16. Tanaka Y, Koyanagi Y, Tanaka R, Kumazawa Y, Nishimura T, Yamamoto N. Productive and lytic infection of human CD4+ type 1 helper T cells with macrophage-tropic human immunodeficiency virus type 1. J Virol 1997; 71:465–70.
17. Suzuki Y, Koyanagi Y, Tanaka Y, et al. Determinant in human immunodeficiency virus type 1 for efficient replication under cytokine-induced CD4+ T-helper 1 (Th1)- and Th2-type conditions. J Virol 1999; 73:316–24.
18. Bosma GC, Custer RP, Bosma MJ. A severe combined immunodeficiency mutation in the mouse. Nature 1983; 301:527–30.
19. Traggiai E, Chicha L, Mazzucchelli L, et al. Development of a human adaptive immune system in cord blood cell-transplanted mice. Science 2004; 304:104–7.
20. Berges BK, Wheat WH, Palmer BE, Connick E, Akkina R. HIV-1 infection and CD4 T cell depletion in the humanized Rag2$^{-/-}\gamma c^{-/-}$ (RAG-hu) mouse model. Retrovirology 2006; 3:76.
21. Ichiyama K, Yokoyama-Kumakura S, Tanaka Y, et al. A duodenally absorbable CXC chemokine receptor 4 antagonist, KRH-1636, exhibits a potent and selective anti-HIV-1 activity. Proc Natl Acad Sci USA 2003; 100:4185–90.
22. Tanaka T, Kitamura F, Nagasaka Y, Kuida K, Suwa H, Miyasaka M. Selective long-term elimination of natural killer cells in vivo by an anti-interleukin 2 receptor beta chain monoclonal antibody in mice. J Exp Med 1993; 178:1103–7.
23. Hunt PW, Harrigan PR, Huang W, et al. Prevalence of CXCR4 tropism among antiretroviral-treated HIV-1–infected patients with detectable viremia. J Infect Dis 2006; 194:926–30.
24. Goldstein H, Pettoello-Mantovani M, Katopodis NF, Kim A, Yurasov S, Kollmann TR. SCID-hu mice: a model for studying disseminated HIV infection. Semin Immunol 1996; 8:223–31.
25. McCune JM. Animal models of HIV-1 disease. Science 1997; 278:2141–2.
26. Aldrovandi GM, Feuer G, Gao L, et al. The SCID-hu mouse as a model for HIV-1 infection. Nature 1993; 363:732–6.
27. Berkowitz RD, Alexander S, Bare C, et al. CCR5- and CXCR4-utilizing strains of human immunodeficiency virus type 1 exhibit differential tropism and pathogenesis in vivo. J Virol 1998; 72:10108–17.
28. Bonyhadi ML, Rabin L, Salimi S, et al. HIV induces thymus depletion in vivo. Nature 1993; 363:728–32.
29. Yokota T, Otsuka T, Mosmann T, et al. Isolation and characterization of a human interleukin cDNA clone, homologous to mouse B-cell stimulatory factor 1, that expresses B-cell- and T-cell-stimulating activities. Proc Natl Acad Sci USA 1986; 83:5894–8.
30. Bonsch D, Kammer W, Lischke A, Friedrich K. Species-specific agonist/antagonist activities of human interleukin-4 variants suggest distinct ligand binding properties of human and murine common receptor gamma chain. J Biol Chem 1995; 270:8452–7.
31. Idzerda RL, March CJ, Mosley B, et al. Human interleukin 4 receptor confers biological responsiveness and defines a novel receptor superfamily. J Exp Med 1990; 171:861–73.
32. Morrison BW, Leder P. A receptor binding domain of mouse interleukin-4 defined by a solid-phase binding assay and in vitro mutagenesis. J Biol Chem 1992; 267:11957–63.